Mutual shielding of neutron activation foils

Ernst Ippel[1,*], *Adri* Paardekooper[1], *Bert* Metz[1], and *Gregor* Bolderink[1]

[1]Nuclear Research and consultancy Group (NRG), 1755 LE Petten, The Netherlands

Abstract. For decommissioning purposes, stacks of foils are used in order to determine the neutron fluence rates in reactor buildings. Due to the relatively great thickness of these foils, self-shielding, as well as mutual shielding become significant for these stacks. In this paper, the results of Monte Carlo calculations are presented for the self-shielding of single foils, and also for the mutual shielding of foils in a stack. Because the irradiation geometry in a reactor building at a large distance from the reactor core is probably not isotropic, especially not so for neutrons of higher energy, the shielding effects were calculated for both isotropic and mono-directional irradiation geometries. The results obtained show a number of general trends which can be understood with a few rules of thumb.

1 Introduction

In recent years, several decommissioning campaigns were conducted in which fluence rate distributions were determined in reactor buildings at considerable distance from the reactor core in order to estimate the levels of activation in structural materials. The fluence rates that are of interest in these campaigns are generally several orders of magnitude smaller than in typical reactor surveillance programs conducted inside or in close proximity to the reactor vessel. If these relatively low fluence rates (or upper boundary thereof) can be demonstrated through measurement, this can significantly reduce the cost associated with dismantling and disposal of materials.

The foil sets used in the decommissioning campaigns were adapted from an existing foil set design that was originally intended for beam characterisation experiments among other things. Because of size restrictions and large neutron fluence gradients present in their original application, this design features a stack of (thin or diluted) foils inside an aluminium holder. For the decommissioning sets, however, thicker, non-diluted foils were employed in the stack in order to obtain the required sensitivity. Furthermore, since the neutron fluence in a reactor building varies from place to place, the foil thickness has to be adjusted accordingly. Therefore, four regions, numbered I, II, III and IV, were defined according to the expected fluence over a one year period. Table 1 shows the configuration of the decommissioning foil sets from front (reactor side) to back together with the corresponding activation reactions, and the boundary values for the expected thermal and fast neutron fluences which define the four fluence regions.

* Corresponding author: Ippel@nrg.eu

Table 1. Order of foils with corresponding activation reaction (left) and fluence ranges (right).

	Target material	Activation reaction
1st	Co or CoAl	$^{59}Co(n,\gamma)^{60}Co$
2nd	Ag or AgAl	$^{109}Ag(n,\gamma)^{110m}Ag$
3rd	Sc or ScAl	$^{45}Sc(n,\gamma)^{46}Sc$
4th	Ni	$^{58}Ni(n,p)^{58}Co$

Region	ϕ_{th}[m^{-2}yr^{-1}]	ϕ_f[m^{-2}yr^{-1}]
I	3.2E+18<ϕ_{th} <3.2E+20	1.6E+18<ϕ_f <3.2E+19
II	3.2E+16<ϕ_{th} <3.2E+18	1.6E+17<ϕ_f <1.6E+18
III	3.2E+15<ϕ_{th} <3.2E+16	3.2E+15<ϕ_f <1.6E+17
IV	3.2E+14<ϕ_{th} <3.2E+15	3.2E+15<ϕ_f <1.6E+17

When the abovementioned stacks of relatively thick, non-diluted foils are used, the effect of both self-shielding and mutual shielding become significant in correctly determining the fluence rates. The main quantity of interest in this paper are the mutual shielding correction factors G of the stacked foils. Formally, the effect of (self-)shielding can be defined as the ratio of the mean fluence rate inside a target volume to the fluence rate on the surface of the target volume. For calculation purposes however, the definition given in Section 2.3 is used.

In addition to the mutual-shielding factors, the self-shielding factors G(d) of some of the foils used in these stacks will be presented as function of thickness d, and the values will be compared with the literature. In some cases, a maximum in G(d), exceeding unity, was observed. For a purely absorbing foil, G-factors are by definition equal to one in a (infinitely) thin or diluted foil, but lower than one in thicker, non-diluted foils. However, when scattering is taken into account, the G-factor can easily become greater than one [1,2,3,4,5,6].

While self-shielding effects in single foils of various thickness can be reasonably well described by elementary approximations [1,7], the analytical description of mutual shielding in a stack of foils is a more complicated problem. Therefore, MCNP simulations were carried out to study this problem, with special consideration of the possible anisotropy of the neutron field present in reactor buildings. For irradiation of foils that are placed inside the reactor core, it is commonly assumed that neutrons of all energies have an isotropic spatial distribution due to the fact that the fuel rods generally are positioned around the foils. For foils placed at a considerable distance outside the core, however, the reactor core can be considered a neutron point source that can locally be approximated by a mono-directional irradiation geometry for higher energy neutrons. Thermal neutrons on the other hand, may have a more isotropic distribution because their thermalisation can be caused by interactions with the building materials in the direct surroundings of the foils. Therefore, both the isotropic and mono-directional spatial neutron distribution will be considered in this paper.

2 MCNP simulations

MCNP simulations were performed with a thermal, an intermediate, and a fast neutron energy spectrum. Moreover, for each neutron energy spectrum, two different spatial neutron distributions were considered; an isotropic distribution and a mono-directional beam. Since in the case of a mono-directional beam the shielding effects depend on the direction in which the foil package is irradiated, the situation in which the package is inadvertently mounted in the reverse orientation has also been investigated. It is well known from the literature that self-shielding for fast neutrons is negligible. Our MCNP simulations showed that this also holds for foils in a stack, so this will not be discussed any further in this paper.

2.1 Neutron spectrum

In the case of commercial decommissioning applications, one often has to resort to the standardised neutron energy distributions due to a lack of knowledge of the spectrum at the positions of the foil stacks. Therefore, the G-factors were calculated for the standardised neutron energy distributions for the thermal, epithermal and fast neutrons separately. Fast neutrons will not be discussed here due to negligible shielding.

2.1.1 Thermal neutrons

For thermal neutrons, the fluence rate distribution is characterised by a Maxwell spectrum:

$$\Phi(E) = C \cdot E \cdot e^{-\frac{E}{kT}} \tag{1}$$

Here k is the Boltzmann constant, and $T = 293.58\ K$ is the absolute temperature that is conventionally chosen to characterise the thermal neutron spectrum . The integration interval ranges from 10^{-10} to $5 \cdot 10^{-7}$ MeV.

2.1.2 Epithermal neutrons

For epithermal neutrons, the fluence rate distribution is characterised by a "1/E" spectrum:

$$\Phi(E) = \frac{1}{E} \tag{2}$$

The integration interval ranges from $5 \cdot 10^{-7}$ to 1 MeV.

2.2 MCNP calculations

For the MCNP calculations, a histogram distribution with energy intervals according to SAND-II has been chosen. For each interval, the probability is calculated according to the respective fluence rate distributions (1) and (2) , which are set to zero outside the integration limits. For the cross-sections, the dosimetry library IRDFF-II [8] has been used. With both the fluence rate and the cross-section as function of energy, MCNP calculates the number of reactions per unit volume (cm^3), according to [9]:

$$R = N \int_{E_{min}}^{E_{max}} \sigma(E)\, \Phi(E) dE \tag{3}$$

where N is the number of atoms per barn·cm.

The neutron (self-)shielding factor $G(d)$ for a target foil with thickness d is defined as the number of reactions $R(d)$ per unit volume, divided by the number of reactions $R(0)$ per unit volume for an infinitely thin foil of the same material:

$$G(d) = \frac{R(d)}{R(0)} \tag{4}$$

$R(d)$ was calculated at a foil thickness d of both 10^{-6} and 10^{-7} cm, which resulted in equal values. Therefore, $R(0)$ is defined as $R(d = 10^{-6})$.

3 Results

The self-shielding factors $G(d)$ were calculated as function of thickness d according to equation (4) for individual Co and Ag target foils to compare the obtained values with

experimental data. Note that for $Sc_{0.019}Al_{0.981}$ and Ni foils, the calculated self-shielding effects are in the order of 1% or less, with no experimental data known for comparison.

3.1 Single foils of various Thickness

3.1.1 Thermal neutrons

As can be seen in Figure 1, the isotropic MCNP calculations are in good agreement with the experimental results for Co and Ag foils found by Freudenreich *et al*. [10], which seems to indicate an isotropic spatial distribution might be a good choice for thermal neutrons.

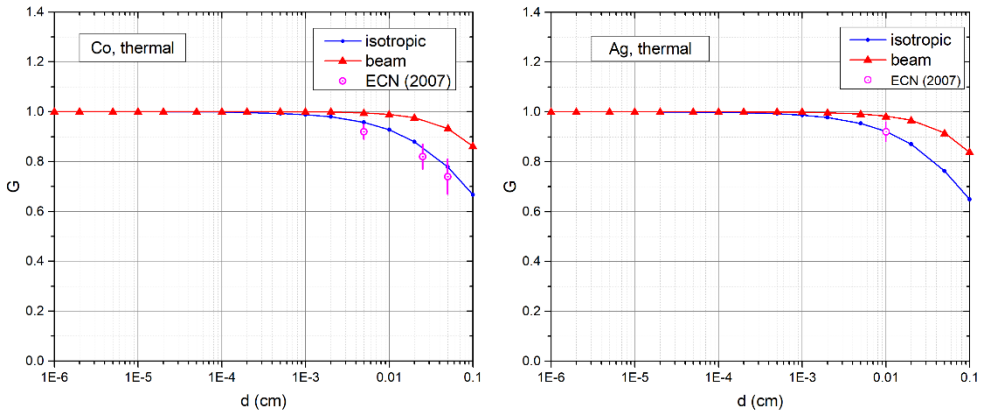

Figure 1. G-factors for Co and Ag foils upon thermal neutron irradiation.

The MCNP calculations presented in Figure 1 were also compared with the analytical approach given in Williams et al. [1], which also takes scattering into account for a beamlike geometry. For the isotropic case, the MCNP calculations agree well with the analytical approach for both Co and Ag (although for Co the values seem to start to diverge for foils with a thickness $d > 0.05$cm). For the beamlike geometry, the calculations agree well with the analytical approach up to a foil thickness of $d = 0.05$cm.

3.1.2 Epithermal neutrons

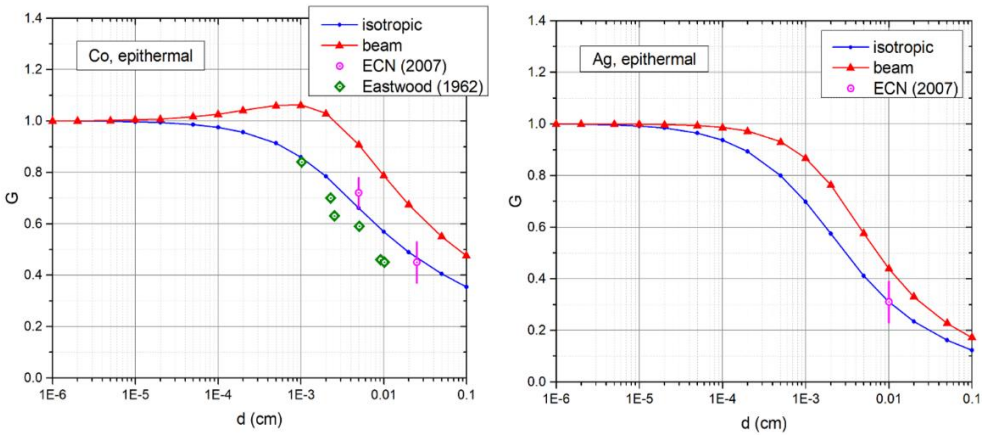

Figure 2. G-factors for Co and Ag foils upon epithermal neutron irradiation.

Similarly, as can be seen in Figure 2, the isotropic MCNP calculations for epithermal neutrons are also in good agreement with the experimental results for Ag and Co foils [10]. Furthermore, a reasonable agreement with experiments by Eastwood *et al*. [11] was found

for Co foils given an isotropic irradiation geometry. This seems to indicate an isotropic spatial distribution might also be a good choice for epithermal neutrons.

The MCNP calculations presented in Figure 2 were not compared with an analytical approach from the literature due to the absence of any analytical approach taking into account scattering for epithermal neutrons.

3.2 Stacks of foils

The thermal and epithermal G-factors for the single foils (G_{SINGLE}) are presented below, both for the beam and isotropic geometry. Furthermore, the G-factors of foils in a stack, both irradiated isotropically (G_{ISO}), and in a beam from the reactor side (G_R) and back side (G_B), are presented.

Table 2. G-factors of stacks of 4 foils upon irradiation with thermal neutrons.

	foil	Material	Thickness (cm)	Radius (cm)	Mono-directional			Isotropic	
					G_{SINGLE}	G_R	G_B	G_{SINGLE}	G_{ISO}
Region I	1st	$Co_{0.001}Al_{0.999}$	0.02	1.0	1.003	1.027	1.004	0.999	0.993
	2nd	$Ag_{0.01}Al_{0.99}$	0.02	1.0	1.003	1.029	1.010	0.999	0.992
	3rd	$Sc_{0.019}Al_{0.981}$	0.01	0.35	1.000	1.037	1.021	1.000	0.989
	4th	Ni	0.01	1.0	-	-	-	-	-
Region II	1st	Co	0.005	1.0	0.996	1.038	0.949	0.957	0.887
	2nd	Ag	0.01	1.0	0.984	1.015	0.988	0.922	0.879
	3rd	$Sc_{0.019}Al_{0.981}$	0.01	1.0	1.000	1.005	1.021	1.000	0.895
	4th	Ni	0.025	1.0	-	-	-	-	-
Region III	1st	Co	0.025	1.0	0.969	1.065	0.862	0.860	0.779
	2nd	Ag	0.01	1.0	0.984	1.026	0.951	0.922	0.773
	3rd	$Sc_{0.019}Al_{0.981}$	0.01	1.0	1.000	1.024	0.989	1.000	0.793
	4th	Ni	0.1	1.0	-	-	-	-	-
Region IV	1st	Co	0.05	1.0	0.933	1.010	0.810	0.778	0.701
	2nd	Ag	0.01	1.0	0.984	0.938	0.945	0.922	0.697
	3rd	Sc	0.01	1.0	1.010	0.935	0.998	0.973	0.721
	4th	Ni	0.1	1.0	-	-	-	-	-

The calculations show that in the case of isotropic thermal neutrons, all foils in a package have almost the same G-factor. It also appears, by comparison with the G-factors of the individual foils, that for the isotropic irradiation geometry the G-factor of a foil in a package can be calculated to a good approximation as the product of the G-factors of the individual foils. Further study (with e.g. a large number of different stacks of materials with and without 1/v cross-sections) is however needed to investigate the generality of this observation. Moreover, although the isotropic thermal G-factors of single foils can thus be calculated to a good approximation by the analytical approach in [1] for the foil thicknesses presented in Table 2, it remains to be seen if the above observation holds in general and therewith if the isotropic analytical expressions can be used for foils of any material placed in a stack. In the case of a thermal beam geometry, the G-factors for single foils show a difference in the order of 1-13% compared to the G-factors of these same foils placed in a stack. Although the thermal beam G-factors of single foils can also be well approximated by the analytical approach in [1] for the foil thicknesses presented in Table 2, this does not necessarily hold for foils in a stack. Also, a significant influence of the orientation of the foil stack in a beam is observed.

Table 3. G-factors for stacks of 4 foils upon irradiation with epithermal neutrons.

	foil	Material	Thickness (cm)	Radius (cm)	Mono-directional			Isotropic	
					G_{SINGLE}	G_R	G_B	G_{SINGLE}	G_{ISO}
Region I	1st	$Co_{0.001}Al_{0.999}$	0.02	1.0	1.005	1.028	1.010	0.999	0.997
	2nd	$Ag_{0.01}Al_{0.99}$	0.02	1.0	0.996	1.022	1.009	0.965	0.965
	3rd	$Sc_{0.019}Al_{0.981}$	0.01	0.35	1.000	1.039	1.026	1.000	1.000
	4th	Ni	0.01	1.0	1.001	1.005	1.008	0.997	0.992
Region II	1st	Co	0.005	1.0	0.908	0.937	0.883	0.661	0.645
	2nd	Ag	0.01	1.0	0.438	0.444	0.436	0.311	0.304
	3rd	$Sc_{0.019}Al_{0.981}$	0.01	1.0	1.000	1.040	1.044	1.000	0.965
	4th	Ni	0.025	1.0	1.001	1.009	1.011	0.994	0.993
Region III	1st	Co	0.025	1.0	0.642	0.695	0.608	0.469	0.454
	2nd	Ag	0.01	1.0	0.438	0.464	0.423	0.311	0.296
	3rd	$Sc_{0.019}Al_{0.981}$	0.01	1.0	1.000	1.149	1.065	1.000	0.950
	4th	Ni	0.1	1.0	1.002	1.016	1.023	0.983	0.986
Region IV	1st	Co	0.05	1.0	0.550	0.596	0.521	0.405	0.394
	2nd	Ag	0.01	1.0	0.438	0.461	0.426	0.311	0.293
	3rd	Sc	0.01	1.0	1.017	1.149	1.095	0.996	0.934
	4th	Ni	0.1	1.0	1.002	1.015	1.026	0.983	0.985

In the case of epithermal neutrons, the G-factors for most of the foils are almost unaffected by the presence of other foils: a foil in a stack has almost the same G-factor as an individual foil. The explanation for this is that most of the activation takes place at the resonance energy, and the resonances of the different reactions hardly overlap. Scandium however lacks a large resonance at low epithermal energy, and therefore shows a deviating trend. If in future literature an analytical approach taking scattering into account is also presented for epithermal neutrons, it could well be that this analytical approach also holds for foils placed in a stack given that the cross-sections of the materials used have large, well-defined and non-overlapping resonances.

As can be seen in Figure 2, and Table 2 and Table 3, the G-factors for a mono-directional irradiation geometry can become larger than 1 for some of the foils, both when irradiated individually and in a stack. Interestingly, this effect seems to be enhanced when foils are placed in a stack. In [1,2], it is shown that G>1 can occur for targets deposited on a backing irradiated in a beam due to (back-)scattering, and they assign this effect to the fact that scattered neutrons, on average, have longer path lengths in the deposit. The self-shielding correction formula they provide, however, does not show a maximum as function of backing (or foil) thickness as is seen in Fig.2. In [3,4], it is shown that G can become greater than unity as a function of thickness d for disks in a beam geometry. This effect is, however, only shown for samples that contain strong scatterers (e.g. hydrogenous materials), but it is mentioned that the enhancement of G depends on both the scattering density and the size and shape of the sample. In [5], it is shown that the epithermal G-factor can become greater than unity as a function of thickness d for samples with low H content (i.e. Cobalt and Manganese), but that this is not the case for gold. In [6], an enhancement of the thermal flux in aqueous samples was observed due to moderation, i.e. down-scattering, of epithermal neutrons. All these observations together seem to indicate that a G-factor larger than one generally results from a combination of elastic, and down-scattering, which in a mono-directional beam leads to both a longer average path length within the foils, and to a neutron energy with a greater corresponding capture probability given an 1/v cross-section relation. For the isotropic case, however, no G-factor larger than unity is observed, which probably

has to do with the fact that the path length does not increase, on average, due to scattering. This explanation seems to be confirmed by the observation that, in all situations, the G-factors for a mono-directional irradiation are equal to or higher than the G-factors for an isotropic irradiation. Considering the purely absorbing case, this can be explained by the fact that neutrons from a mono-directional distribution, on average, come across fewer target atoms because they impinge perpendicular to the surface of the foils. Taking scattering into account, the number of target atoms neutrons from an isotropic distribution come across remains, on average, approximately the same, and the only effect that could raise the value of G is down-scattering. Neutrons from a mono-directional distribution, however, experience down-scattering, but also come across more target atoms due to scattering, so the rise in G due to (down-)scattering will always be higher in the mono-directional case. Scattering thus magnifies the difference in G-factors for the isotropic versus the mono-directional case.

4 Discussion

The influence of the spatial neutron distribution on the G-factors of single foils is well described in the literature. This influence can also be seen in Figure 1 and Figure 2. Furthermore, looking at Table 2 and Table 3, it appears that the influence of the spatial distribution becomes even more significant for these same foils packed in a stack. It is therefore important to have an idea about which spatial distribution to use in decommissioning applications. Although the isotropic thermal and epithermal G-factors of the individual Co and Ag foils calculated with MCNP seem to be in reasonably good agreement with the experimentally determined G-factors, the experimental G-factors were not determined inside a reactor building at a considerable distance from the reactor core. Therefore, especially for the epithermal neutrons, it remains to be seen whether the spatial neutron distribution farther from the core is indeed purely isotropic, or if there might be a preferred spatial direction. This could be investigated with MCNP simulations in which the spatial distribution of epithermal neutrons outside the biological shield is analysed as a function of biological shield thickness for general nuclear power plant designs (i.e. a core surrounded by [heavy] water and concrete). These simulations might lead to general guidelines for the use of spatial distributions in decommissioning applications.

5 Conclusions

For single foils of various thickness, the calculations agree well with the available experimental data found in the literature. Moreover, the calculations for thermal neutrons agree well with the analytical approach in [1] up to a foil thickness of d = 0.05cm. For stacks of foils, the main results in this paper can be summarized as follows:

- A significant difference in the G-factors of single foils vs. these same foils in a stack is observed for thermal neutrons, implying analytical expressions for thermal self-shielding from the literature cannot simply be applied to foils placed in a stack. For epithermal neutrons the difference is much less significant (especially for materials with well-defined, non-overlapping resonance peaks), meaning analytical expressions for single foils could possibly be used to approximate the G-factors of these foils in a stack.
- A significant difference in both the thermal and epithermal G-factors is observed for an isotropic vs. mono-directional beam irradiation geometry. This is well-known in the literature for single foils and can be shown analytically[1,7]. For a stack of foils, although harder to show analytically, this still holds, which is in line with our expectations. Furthermore, the influence of the spatial neutron distribution on the G-factors becomes more significant for foils placed in a stack.

- In the thermal energy region, the G-factors of all foils in an isotropically irradiated stack (last column of Table 2) have approximately the same value, which is approximately equal to the product of the G-factors of the individual foils (second-last column of Table 2). Future work is needed to show if this holds in general.
- In the thermal energy region, the G-factors of mono-directionally irradiated foils are decreasing with their distance from the entry surface, which can be explained by simple exponential attenuation arguments due to the 1/v cross-section relation in this energy region.
- In the epithermal energy region, the G-factors of all but the scandium foils in a stack tend to keep their individual values, irrespective of the presence of other foils. This effect is likely due to the fact that the neutron resonances in the different foils hardly overlap, except for scandium, which only has a large number of smaller, consecutive resonances at energies higher than that of the main resonance of cobalt and silver.

6 Outlook

Based on the discussion, it is recommended to further investigate the spatial neutron distribution in a reactor building to get a better understanding of the relative importance of mono-directional vs. isotropic irradiation geometries. The goal of this investigation should be to obtain general guidelines that can be used in the choice of the correct spatial distribution in situations applicable to decommissioning circumstances, i.e. outside biological shields of general nuclear power plants designs.

References

1. J.G. Williams and D.M. Gilliam, Thermal neutron standards, Metrologia 48 S254, DOI 10.1088/0026-1394/48/6/S03 (2011)
2. R.D. Scott et al., The characterisation of 10B and 6LiF reference deposits by the measurement of neutron induced charged particle reactions, Nuclear Instruments and Methods in Physics Research A314 (1992) 163-170, North Holland
3. E.A. Mackey and J.R.D. Copley, Scattering and absorption effects in neutron beam activation analysis experiments, Journal of Radioanalytical and Nuclear Chemistry, Articles, Vol. 167, No.1 (1993) 127-132
4. J.R.D. Copley and C.A. Stone, Neutron scattering and its effect on reaction rates in neutron absorption experiments, Nuclear Instruments and Methods in Physics Research A281 (1989) 593-604
5. I.F. Gonçalves, E. Martinho and J. Salgado, Monte Carlo calculation of resonance self-shielding factors for epithermal neutron spectra, Radiation Physics and Chemistry 61, p.461-462 (2001).
6. S.A. Reynolds and W.T. Mullins, Neutron flux perturbation in activation analysis, International Journal of Applied Radiation and Isotopes (1963) Vol.14, pp, 421-425
7. Neutron Fluence Measurements, *Technical Report Series 107*, IAEA, Vienna, (1970), STI/DOC/10/107
8. A. Trkov et al., IRDFF-II: A New Neutron Metrology Library, Nuclear Data Sheets 163, p.1-108, (2020)
9. R.C. Little and R.E. Seamon, Dosimetry/Activation Cross Sections for MCNP, LANL Internal Memorandum, (1984)
10. W.E. Freudenreich and J.I. Wolters, Empirical Determination of Thermal and Epithermal Neutron (Self)-Shielding Correction Factors for Thick Cobalt and Silver Activation Monitors, NRG-report 22052/07.82495, (unpublished) (2007)
11. T.A. Eastwood and R.D. Werner. Resonance and Thermal Neutron Self-Shielding in Cobalt Foils and Wires, Nuclear Science and Engineering 13, p. 385-490, (1962)